

Conditions for Feedback Linearization of Network Systems

Tommaso Menara^{ID}, *Student Member, IEEE*, Giacomo Baggio^{ID}, *Member, IEEE*, Danielle S. Bassett^{ID},
and Fabio Pasqualetti^{ID}, *Member, IEEE*

Abstract—Feedback linearization allows for the local transformation of a nonlinear system to an equivalent linear one by means of a coordinate transformation and a feedback law. Feedback linearization of large-scale nonlinear network systems is typically difficult, since existing conditions become harder to check as the network size becomes larger. In this letter, we provide novel conditions to test whether a nonlinear network is feedback-linearizable. Specifically, given some dedicated control inputs injected to a set of network nodes, we derive an easy-to-check algebraic condition that can be tested on the Jacobian matrix of the network dynamics evaluated at some desired working point. Furthermore, our requirements are sufficient for (local) controllability, and thus provide a testable condition for controllability of large-scale nonlinear networks. Finally, we validate our findings by enforcing the formation of desired synchronization patterns in networks of coupled oscillators.

Index Terms—Control of networks, feedback linearization, algebraic/geometric methods.

I. INTRODUCTION

THE ABILITY to effectively control complex nonlinear systems is still an outstanding engineering challenge. In fact, despite the ubiquitous presence of large-scale nonlinear network systems, both in the technological [1] and the natural [2] fields, a full characterization of controllability

has remained elusive. This is due to the fact that, in general, checking the known sufficient conditions becomes harder (intractable, even) as the size of the system increases [3]. In this letter, we address this issue by providing algebraic conditions for nonlinear control problems that leverage the system's internal interconnection structure. Specifically, we resort to the theory of feedback linearization, which allows for the local transformation of a nonlinear system into an equivalent linear one by means of a coordinate transformation and a feedback loop [4]. This, in turn, enables the extensive array of control-theoretic tools for linear systems to be used for the control of nonlinear network systems.

While there exists a vast amount of literature on controllability of linear systems evolving on networks, the line of work studying the nonlinear counterpart is much narrower (e.g., [5], [6]). This letter complements the latter line of work and presents conditions to test whether a nonlinear network system is feedback-linearizable from a set of dedicated control inputs. Our conditions can be evaluated on the Jacobian matrix of the system computed at a desired working point, instead of complex differential geometric quantities as in classical tests, which also consist of more restrictive conditions. Finally, motivated by our interest in controlling the synchronization capabilities of neuronal networks in biological systems, we illustrate how our results can be used to achieve cluster synchronization in regular and multiplex networks of oscillatory neuronal ensembles [7], [8].

Related Work: This letter aims at narrowing the gap between controllability of large-scale network systems and the feedback linearization method. After the early theoretical developments, fewer works have surfaced on the topic of nonlinear controllability, [9], [10]. Recent papers address this problem for systems evolving on networks [5], [6], [11]–[14]. For instance, [13], [14] study accessibility of network systems. However, accessibility is a weaker notion than controllability, and thus may be of limited use in practice [15].

Feedback linearization is a classical topic in nonlinear control theory developed during the decades between the 1960 and the 1990 [16], [17]. Applications can be found in several engineering systems, including robotic mechanisms [18] and power networks [19]. Some recent work promotes the usage of data-driven methods to achieve feedback linearization whenever the model is not known exactly [20], [21]. Relevant

Manuscript received January 9, 2020; revised March 11, 2020; accepted March 12, 2020. Date of publication March 17, 2020; date of current version April 3, 2020. This work was supported in part by Award ARO71603NSYIP, Award NSF-NCS-FO-1631112, Award NSF-NCS-FO-1926829, and Award AFOSR-FA9550-19-1-0235. Recommended by Senior Editor M. Arcak. (*Corresponding author: Tommaso Menara.*)

Tommaso Menara and Fabio Pasqualetti are with the Department of Mechanical Engineering, University of California at Riverside, Riverside, CA 92612 USA (e-mail: tomenara@engr.ucr.edu; fabiopas@engr.ucr.edu).

Giacomo Baggio is with the Department of Information Engineering, University of Padova, 35131 Padua, Italy (e-mail: baggio@dei.unipd.it).

Danielle S. Bassett is with the Department of Bioengineering, University of Pennsylvania, Philadelphia, PA 19104 USA, also with the Department of Electrical and Systems Engineering, University of Pennsylvania, Philadelphia, PA 19104 USA, also with the Department of Physics and Astronomy, University of Pennsylvania, Philadelphia, PA 19104 USA, also with the Department of Psychiatry, University of Pennsylvania, Philadelphia, PA 19104 USA, and also with the Department of Neurology, University of Pennsylvania, Philadelphia, PA 19104 USA (e-mail: dsb@seas.upenn.edu).

Digital Object Identifier 10.1109/LCSYS.2020.2981339

studies on model-based feedback linearization include [22], where the authors give conditions based on differential geometry, and [23], where conditions are given for a single-input-single-output system with delays. The work that is most closely related to ours is [19], where the authors study feedback linearization of a chain network governed by a class of nonlinear dynamics.

Paper Contribution: The contribution of this letter is two-fold. First, by exploiting a system's interconnected structure, we provide sufficient algebraic conditions to test for the feedback linearization of nonlinear systems controlled by linear vector fields. That is, given a set of dedicated control inputs, we derive conditions that can be tested on the Jacobian matrix of the nonlinear system. Our conditions can be used to test for (local) controllability of large-scale nonlinear network systems. Additionally, the use of feedback linearization enables the evaluation of the state space region in which the linearized system is defined; note that this is a computation not possible when using Jacobian linearization.

Second, we exploit our results to address the challenging problem of controlling oscillatory networks [8], [24], [25]. We show that a class of nonlinearly coupled oscillators is feedback-linearizable and, through feedback linearization, we control the formation of desired synchronization patterns.

II. PROBLEM SETUP AND PRELIMINARY NOTIONS

In this letter, we study feedback linearization and controllability of nonlinear systems governed by the dynamics

$$\dot{x} = f(x) + Bu, \quad (1)$$

where $x = [x_1, \dots, x_n]^T \in \mathbb{R}^n$ is the system state, f is a smooth vector field that describes the dynamics of the system, and $B \in \mathbb{R}^{n \times m}$ is the input matrix through which the control signals u are administered to the system. We let $\mathcal{K} = \{k_1, \dots, k_m\} \subseteq \{1, \dots, n\}$ be the control set, and let $B = [e_{k_1}, \dots, e_{k_m}]$, with e_i denoting the i -th canonical vector. Without loss of generality, we choose $\mathcal{K} = \{1, \dots, m\}$, thus $B = [e_1, \dots, e_m]$. Finally, we assume that (1) has at least one equilibrium. That is, there exists \bar{x} such that $f(\bar{x}) = 0$.

In this letter, we make use of a graphical representation of the dynamic interdependence of the system's components. Namely, the *inference diagram* [26] consists of a graph $\mathcal{G} = (\mathcal{V}, \mathcal{E})$, with $\mathcal{V} = \{1, \dots, n\}$ being the set of n nodes where each node corresponds to a state of the system, and $\mathcal{E} \subseteq \mathcal{V} \times \mathcal{V}$ being the set of edges connecting the nodes as follows. For all $i, j \in \mathcal{V}$, there exists an unweighted directed edge from node j to node i if $i \neq j$ and x_j appears in x_i 's differential equation. The adjacency matrix that describes the interconnection structure of the inference diagram is the sparse matrix $A = [a_{ij}]$, with $a_{ij} = 1$ if there is an edge between j and i , and $a_{ij} = 0$ otherwise. Fig. 1 illustrates the procedure to generate an inference diagram, which describes the underlying topology of the state interactions for the nonlinear system $\dot{x} = f(x)$ in (1), but can equivalently represent the interconnection structure of nonlinearly interacting agents in a network system.

Let A be the adjacency matrix of \mathcal{G} , let $\text{path}(i, j)$ denote a path on \mathcal{G} from node i to node j , and let $|\text{path}(i, j)|$

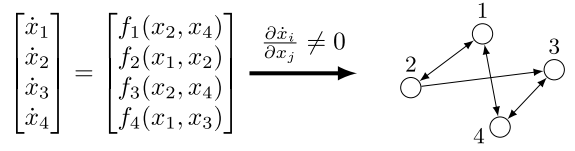


Fig. 1. This figure illustrates the process of generating an inference diagram from a generic nonlinear system described by the vector field $f(x)$. The inference diagram depicted in this example is a graph in which there is an edge from node j to node i if \dot{x}_i is a function of x_j and $i \neq j$. Notice that we do not allow self-loops in the inference diagram.

be the number of edges of $\text{path}(i, j)$. Notice that \mathcal{K} represents the set of control nodes in \mathcal{G} . Define the distance between a subset of nodes $\mathcal{S} \subseteq \mathcal{V}$ and the control set \mathcal{K} as $\text{dist}(\mathcal{S}, \mathcal{K}) = \min\{|\text{path}(i, j)| : i \in \mathcal{K}, j \in \mathcal{S}\}$. Without loss of generality, we order the nodes according to their distance from the set of control nodes. In particular, we define a positive integer N so that $\mathcal{V} = \bigcup_{i=1}^N \mathcal{V}_i$, with $\mathcal{V}_i \cap \mathcal{V}_j = \emptyset$ if $i \neq j$, and $\text{dist}(\mathcal{V}_i, \mathcal{K}) = i - 1$ for all $i \in \{1, \dots, N\}$. According to the partition $\{\mathcal{V}_1, \dots, \mathcal{V}_N\}$, the adjacency matrix reads as

$$A = \begin{bmatrix} A_{11} & A_{12} & 0 & \cdots & 0 \\ A_{21} & A_{22} & A_{23} & \cdots & 0 \\ 0 & A_{32} & \ddots & \ddots & \vdots \\ \vdots & \ddots & \ddots & A_{N-1, N-1} & A_{N-1, N} \\ 0 & \cdots & \cdots & A_{N, N-1} & A_{N, N} \end{bmatrix}, \quad (2)$$

where $A_{ii} \in \mathbb{R}^{|\mathcal{V}_i| \times |\mathcal{V}_i|}$, $A_{i-1, i} \in \mathbb{R}^{|\mathcal{V}_i| \times |\mathcal{V}_{i-1}|}$, and $A_{i, i-1} \in \mathbb{R}^{|\mathcal{V}_{i-1}| \times |\mathcal{V}_i|}$, with $|\mathcal{V}_i|$ denoting the cardinality of \mathcal{V}_i .

In this letter, we address the following problem, whose solution is intimately tied to finding conditions for the local controllability of nonlinear systems.¹ Given a nonlinear system in the form (1), we investigate whether there exists a state feedback control law $u = \alpha(x) + \beta(x)v$ and a change of coordinates $z = \Phi(x)$ that transform the nonlinear system (1) into an equivalent controllable linear system of the form

$$\dot{z} = A_{\text{lin}} z + B_{\text{lin}} v,$$

where $A_{\text{lin}} \in \mathbb{R}^{n \times n}$ and $B_{\text{lin}} \in \mathbb{R}^{n \times m}$.

To answer this question, we will make use of some notions from geometric control theory [3], [27]. Given two vector fields $f(x)$ and $g(x)$, both defined in an open subset of \mathbb{R}^n , we define the operation $[f, g]$ as the *Lie bracket* between $f(x)$ and $g(x)$, which yields the smooth vector field

$$[f, g](x) = \frac{\partial g(x)}{\partial x} f(x) - \frac{\partial f(x)}{\partial x} g(x).$$

To avoid confusing notation such as $[f, [f, \dots, [f, g]]]$, we use the following recursive definition:

$$\text{ad}_f^k g(x) = [f, \text{ad}_f^{k-1} g](x),$$

where $\text{ad}_f^0 g(x) = g(x)$. Note that the directions in which the state may be moved around an initial condition are those belonging to the set of all vector fields that can be obtained by

¹A system in the form (1) is locally controllable at \bar{x} if there exists a neighborhood $\mathcal{B}_{\bar{x}}$ of \bar{x} such that for all $x_f \in \mathcal{B}_{\bar{x}}$, there exist $T > 0$ and a control input u that brings $x(0) = \bar{x}$ to $x(T) = x_f$.

iteratively computing the Lie brackets of the system's dynamics and the control vector fields. Further, given a real-valued function $\lambda(x)$ and a vector field $f(x)$, both defined in an open set of \mathbb{R}^n , we define the *derivative of λ along f* :

$$L_f \lambda(x) = \frac{\partial \lambda(x)}{\partial x} f(x).$$

If the function λ is differentiated k times along f , we write

$$L_f^k \lambda(x) = \frac{\partial (L_f^{k-1} \lambda(x))}{\partial x} f(x).$$

For the sake of simplicity, we will omit the argument x when it is clear from the context. A (smooth) *distribution* is the assignment of the subspace spanned by the values at x of some smooth vector fields f_1, \dots, f_d that are defined in an open set $\mathcal{X} \subseteq \mathbb{R}^n$, and is denoted by $\mathcal{G} = \text{span}\{f_1, \dots, f_d\}$. In other words, a distribution assigns a vector space to each point x of the set \mathcal{X} . A distribution \mathcal{G} is involutive if, whenever $f, g \in \mathcal{G}$, also $[f, g] \in \mathcal{G}$. Finally, the distribution \mathcal{G} has constant dimension in a set $\mathcal{X} \subseteq \mathbb{R}^n$ whenever its dimension remains the same at all points in \mathcal{X} .

III. STRUCTURAL CONDITIONS FOR FEEDBACK LINEARIZATION

In this section, we show that if the inference diagram of a nonlinear system belongs to a well-defined class of networks, then there exists a change of coordinates such that the original controlled nonlinear system (1) can be transformed into a controllable linear system by means of a feedback law. Clearly, these conditions constitute a sufficient test for local controllability of nonlinear systems.

Before presenting our results, notice that the Jacobian $J(x) = \frac{\partial f(x)}{\partial x}$ of (1) reads as

$$J(x) = \begin{bmatrix} D_1(x) & U_1(x) & 0 & \cdots & 0 \\ L_1(x) & D_2(x) & U_2(x) & \cdots & 0 \\ 0 & L_2(x) & \ddots & \ddots & \vdots \\ \vdots & \ddots & \ddots & D_{N-1}(x) & U_{N-1}(x) \\ 0 & \cdots & \cdots & L_{N-1}(x) & D_N(x) \end{bmatrix}, \quad (3)$$

where the blocks have the same size of the blocks in the matrix A in (2). We are now ready to present our main result.

Theorem 1 (Condition for Feedback Linearization): Consider the dynamics (1). Let \bar{x} be such that $f(\bar{x}) = 0$ and let the Jacobian $J(x) = \frac{\partial f(x)}{\partial x}$ read as in (3). The system is feedback-linearizable at \bar{x} if $\text{rank}(L_i(\bar{x})) = |\mathcal{V}_{i+1}|$ for all $i = \{1, \dots, N-1\}$.

Theorem 1 implicitly requires a certain network structure to hold true, as we elucidate in the following remark.

Remark 1 (Necessary Network Structure for the Condition in Theorem 1): Theorem 1 requires the subdiagonal blocks of $J(\bar{x})$ to be full row rank. Note that a necessary condition for this to hold true is that $|\mathcal{V}_{i+1}| \leq |\mathcal{V}_i|$ for all $i \in \{1, \dots, N-1\}$ (see Fig. 2 for an example). Furthermore, every node in partition \mathcal{V}_{i+1} must have at least one incoming connection from nodes in \mathcal{V}_i . Clearly, this interconnection requirement

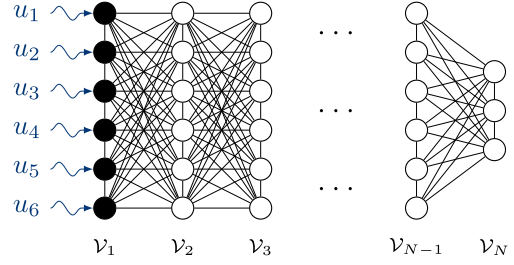


Fig. 2. Network system with tridiagonal adjacency matrix as in (2) and node partition satisfying $|\mathcal{V}_1| \leq |\mathcal{V}_2| \leq \dots \leq |\mathcal{V}_N|$. Examples of networks with this topology are artificial neural networks, multiplex networks and, in general, all grid-like networks with layers of equal or decreasing cardinality.

prevents the network topology to produce zero rows in $L_i(\bar{x})$ for all $i \in \{1, \dots, N-1\}$.

Before proving Theorem 1 we introduce a lemma that relates the distribution of the Lie brackets of the dynamics (1) to the image of a block triangular matrix.

Lemma 1 (Block Upper Triangular Distribution): Consider the dynamics (1). Let $\mathcal{G}_k = \text{span}\{\text{ad}_f^r e_\ell : 0 \leq r \leq k, 1 \leq \ell \leq m\}$, $k \in \{0, \dots, N-1\}$. The distribution $\mathcal{G}_k(x)$ can be written as

$$\mathcal{G}_k(x) = \text{Im} \begin{bmatrix} E_{1,1}(x) & \otimes & \cdots & \otimes \\ 0 & E_{2,2}(x) & \cdots & \vdots \\ \vdots & \ddots & \ddots & \otimes \\ 0 & \cdots & 0 & E_{k+1,k+1}(x) \\ 0 & \cdots & 0 & 0 \end{bmatrix},$$

$\underbrace{\hspace{10em}}_{G_k(x)}$

where Im denotes the image of a matrix, $G_0(x) = B$, so that $E_{1,1}(x) = I$, $E_{i,i}(x) = L_{i-1}(x)E_{i-1,i-1}(x) \in \mathbb{R}^{|\mathcal{V}_i| \times |\mathcal{V}_i|}$, \otimes is any real matrix-valued function of x of suitable dimension, and 0 is a zero matrix of suitable dimension.

Proof: Consider first $\mathcal{G}_0(x)$, and notice that, since $\text{ad}_f^0 e_\ell = e_\ell$, for $\ell = 1, \dots, m$, $G_0(x) = [e_1, \dots, e_m] = B$. Next, because of the definition of $\mathcal{G}_k(x)$, at each new step $k \in \{1, \dots, N-1\}$, m new vector fields of the form

$$\text{ad}_f^k e_\ell = \frac{\partial \text{ad}_f^{k-1} e_\ell}{\partial x} f - \frac{\partial f}{\partial x} \text{ad}_f^{k-1} e_\ell, \quad (4)$$

with $\ell = 1, \dots, m$, add to $\{\text{ad}_f^r e_\ell : 0 \leq r < k, 1 \leq \ell \leq m\}$ to generate the distribution $\mathcal{G}_k(x)$. The space spanned by these new vector fields corresponds to the space spanned by the last $|\mathcal{V}_{k+1}|$ columns of $G_k(x)$, which encompass the block $E_{k+1,k+1}(x)$. In what follows we show that, because of the (block) tridiagonal structure of A , only the second part of (4) contributes to the definition of these columns, and, therefore, of the block $E_{k+1,k+1}(x)$. To see this, consider the Lie bracket $\text{ad}_f^k e_\ell(x)$ and notice that its first term reads as

$$\begin{aligned} \left[\frac{\partial \text{ad}_f^{k-1} e_\ell}{\partial x} f \right](x) &= \begin{bmatrix} M_1 & 0 \\ 0 & 0 \end{bmatrix} f(x) \\ &= [\underbrace{\otimes \cdots \otimes}_{\tilde{n}} 0 \cdots 0]^T, \end{aligned}$$

where M_1 is $\tilde{n} \times \tilde{n}$, with $\tilde{n} = \sum_{i=1}^k |\mathcal{V}_i|$. Note that the definition of \tilde{n} follows from the node labeling and the fact that, for all $j \in \{1, \dots, N-1\}$, the nodes in \mathcal{V}_j can only be connected with at most $|\mathcal{V}_{j+1}|$ nodes in \mathcal{V}_{j+1} . Thus, since the first term of each Lie bracket (4) does not affect the last $|\mathcal{V}_{j+1}|$ entries of the second term, the equation $E_{j,j}(x) = L_{j-1}(x)E_{j-1,j-1}(x)$ follows by direct computation of the second term in (4), and the claimed statement follows. ■

In brief, the result in Lemma 1 states that each new $\mathcal{G}_k(x)$ “discovers” $|\mathcal{V}_{k+1}|$ new columns of $G_k(x)$ containing the entries of the block $E_{k+1,k+1}(x)$. We use this finding to prove our main result.

Proof Theorem 1: For some nonnegative integer k , we let $\mathcal{G}_k = \text{span}\{\text{ad}_f^r e_\ell : 0 \leq r \leq k, 1 \leq \ell \leq m\}$. The system (1) is feedback-linearizable if and only if the following three conditions hold [3, Th. 5.2.3]:

- 1) \mathcal{G}_{n-1} has dimension n at \bar{x} ;
- 2) for each $0 \leq k \leq n-1$, \mathcal{G}_k has constant dimension in a neighborhood of \bar{x} ; and
- 3) for each $0 \leq k \leq n-2$, \mathcal{G}_k is involutive,

where $n = |\mathcal{V}|$. Condition 1) follows directly from Lemma 1 and from the assumption $\text{rank}(L_i(\bar{x})) = |\mathcal{V}_{i+1}|$ by noticing that each diagonal block $E_{i,i}(\bar{x})$ is full rank for all $i \in \{1, \dots, k+1\}$. More in detail, let $P \in \mathbb{R}^{n_1 \times n_2}$ and $Q \in \mathbb{R}^{n_2 \times n_2}$; the fact $\text{rank}(PQ) = \text{rank}(P)$ if $\text{rank}(Q) = n_2$ implies the full rank of $E_{i,i}(\bar{x}) = L_{i-1}(\bar{x})E_{i-1,i-1}(\bar{x})$.

In regards to condition 2), from the assumption $\text{rank}(L_i(\bar{x})) = |\mathcal{V}_{i+1}|$, the continuity of singular values, and the definition of $E_{i,i}$ in Lemma 1, it follows that the blocks $E_{i,i}(x)$ are full row rank in a neighborhood of \bar{x} . Thus, in such a neighborhood, the definition of the matrix G_k ensures that the dimension of \mathcal{G}_k , for each $0 \leq k \leq n-1$, remains constant, and condition 2) holds.

Finally, to show that condition 3) holds, we observe that due to the structure of $\mathcal{G}_k(x)$ in Lemma 1, the Lie brackets between any two vector fields in $\mathcal{G}_k(x)$, $0 \leq k \leq N-1$, cannot have nonzero rows greater than $\tilde{n} = \sum_{i=1}^{k+1} |\mathcal{V}_i|$. Thus, the Lie bracket $\text{ad}_f^{j-1} e_\ell$ can only contain states up to \tilde{n} , and $\mathcal{G}_k(x)$ must be involutive for all $0 \leq k \leq N-1$. Note that, for $k > N-1$, \mathcal{G}_k clearly remains involutive. This concludes the proof. ■

A few comments are in order. First, Theorem 1 is constructive, can be used to check whether a network is feedback-linearizable, and also to design networks that satisfy such a property. Second, Theorem 1 implies that there exist a linearizing feedback of the form $u = \alpha(x) + \beta(x)v$ and a diffeomorphism $z = \Phi(x)$ that solve the state-space exact linearization problem [3, Sec. 5.2]. That is, it is possible to transform (1) into an equivalent linear system $\dot{z} = A_{\text{lin}}z + B_{\text{lin}}v$ with $\text{rank}[B_{\text{lin}} \ A_{\text{lin}}B_{\text{lin}} \ \dots \ A_{\text{lin}}^{n-1}B_{\text{lin}}] = n$. Thus, being the pair $(A_{\text{lin}}, B_{\text{lin}})$ controllable, Theorem 1 can also be used to assess local controllability of (1) at \bar{x} .

Corollary 1 (Condition for Nonlinear Controllability): Consider the dynamics (1), and let \bar{x} be such that $f(\bar{x}) = 0$. If the lower diagonal blocks $L_i(\bar{x})$, $i = \{1, \dots, N-1\}$, of the Jacobian (3) have full row rank, then the system (1) is locally controllable at \bar{x} .

Notice that, because the linear system $\dot{z} = A_{\text{lin}}z + B_{\text{lin}}v$ is defined in an open set that depends on the nonlinear

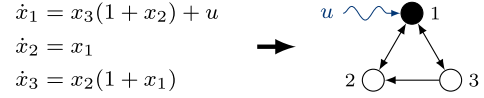


Fig. 3. This figure illustrates the inference diagram obtained from the system in Example 2. The controlled node, which corresponds to x_1 , is filled in black. Since $|\{2,3\}| > |\{1\}|$, the condition in Theorem 1 cannot be satisfied. Yet, the system is feedback-linearizable, as we show in Example 2.

feedback and change of coordinates, we can evaluate the size of the region of the state space in which the linear transformation holds. In fact, if $\Phi(x)$, $\alpha(x)$, and $\beta(x)$ are defined in an open neighborhood \mathcal{U} of \bar{x} , then the linear system is defined in the open set $\Phi(\mathcal{U})$. This fact enables the exact characterization of the operating regions for the feedback-linearized system. Conversely, Jacobian linearization is only exact at the equilibrium point at which the Jacobian matrix is computed. It is also worth noting that Jacobian linearization does not yield the same system as the feedback-linearized one.

Example 1 (Difference in Local Controllability Between Jacobian and Feedback Linearization): Consider the system (1), with $f(x) = [0 \ x_1 \ x_2 + x_1^2/2]^T$ and $b = e_1$. It is easy to see that the controllability matrix of the linearized system at the origin is full rank. Thus, the system is locally controllable around $\bar{x} = [0 \ 0 \ 0]^T$. Yet, since the distribution $\mathcal{G}_1(x) = \text{span}\{e_1, [f, e_1]\}$ is not involutive, by [3, Th. 5.2.3], the system is not feedback-linearizable at \bar{x} .

It should be noted that the condition in Theorem 1 enables a general structural approach to assess feedback-linearizability of nonlinear systems with dynamics (1). Yet, it is only sufficient, as we show in the next example.

Example 2 (Non-necessity of Theorem 1): Consider the system in Fig. 3 with control vector $b = e_1$. Notice that such a system does not satisfy Theorem 1 at $\bar{x} = 0$. Yet, it can be verified that the matrix² $G_2(\bar{x}) = \{b, [f, b], [f, [f, b]]\}(\bar{x}) = \text{diag}(1, -1, 1)$, is full rank, and that $\mathcal{G}_2 = \text{span}\{b, [f, b]\} = [\begin{smallmatrix} 1 & 0 & 0 \\ 0 & -1 & x_2 \end{smallmatrix}]^T$ is involutive. Thus, by [3, Th. 5.2.3], this system is feedback linearizable at the origin.

IV. APPLICATION TO CLUSTER SYNCHRONIZATION OF NONLINEARLY COUPLED OSCILLATORS

In this section, we apply the results developed in Section III to the important problem of controlling the emergence of clusters of neural units with synchronized activity. Specifically, we use feedback linearization to divide networks of nonlinear oscillators into distinct synchronized groups. We achieve this goal without resorting to the prescriptive conditions required by previous work [28], [29].

A. Network of Kuramoto Dynamics

Patterns of correlated activity among neural units play a role in the correct execution of cognitive functions and in the abnormal dynamics of a class of neurological disorders, such as Parkinson’s disease and epilepsy [30], [31]. A classical model used to represent the oscillatory behavior of

²We denote with $\text{diag}(\cdot)$ a diagonal matrix.

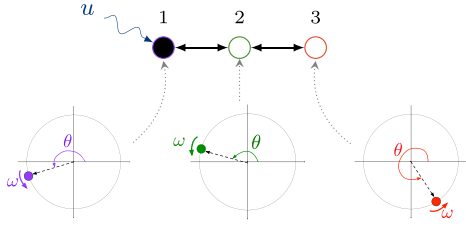


Fig. 4. This figure represents the network of oscillators studied in Section IV-A. Each node represents an oscillator, whose dynamics are defined by the natural frequency ω and the interactions with neighboring oscillators. The first node receives the control input u , and is filled in black to represent $\mathcal{K} = \{1\}$. We choose a simple topology because it allows us to easily illustrate the results of Section III, which can be extended to larger systems.

brain activity is the Kuramoto model of diffusively-coupled oscillators [8], [32]. The dynamics of the i -th oscillator is

$$\dot{\theta}_i = \omega + \sum_{j \neq i} h_{ij} \sin(\theta_j - \theta_i), \quad (5)$$

where ω represents the natural frequency of the oscillators, θ_i is the phase of the i -th oscillator, and $h_{ij} \in \mathbb{R}_{>0}$ denotes the coupling strength between interconnected oscillators, with $\mathbb{R}_{>0}$ indicating the set of positive real numbers.

Interconnected systems of diffusively-coupled oscillators evolve on a network that is described by a weighted adjacency matrix $H = [h_{ij}]$, where $h_{ij} \in \mathbb{R}_{>0}$ if $(j, i) \in \mathcal{E}$, and $h_{ij} = 0$ otherwise. Here, we choose the vector field

$$f(\theta) = \begin{bmatrix} \omega + h_{12} \sin(\theta_2 - \theta_1) \\ \omega + h_{21} \sin(\theta_1 - \theta_2) + h_{23} \sin(\theta_3 - \theta_2) \\ \omega + h_{32} \sin(\theta_2 - \theta_3) \end{bmatrix},$$

where $h_{12} = h_{21} = 1$, $h_{23} = h_{32} = 2$, and the control input is injected into the first oscillator through a control vector field $b = [1 \ 0 \ 0]^T$. It is worth noting that for all diffusively-coupled oscillators, the inference diagram is also described by the adjacency matrix H after all weights are binarized.³ The adjacency matrix for this illustrative example reads as $A = [e_2, e_1 + e_3, e_2]$, and the network is depicted in Fig. 4.

With the aid of a rotating reference frame with angular velocity ω , we can study the equilibria of (5) as fixed points. We choose to stabilize the unstable equilibrium $\bar{\theta} = [\pi \ \pi \ 0]^T$, but we remark that this network satisfies Theorem 1 at all equilibria. We start the derivation of the linearizing feedback law from the Lie brackets $\text{ad}_f b$ and $\text{ad}_f^2 b$, which read as $\text{ad}_f b = [h_{12} \cos(\theta_2 - \theta_1) \quad -h_{21} \cos(\theta_1 - \theta_2) \quad 0]^T$, and

$$\text{ad}_f^2 b = \begin{bmatrix} h_{12}(h_{12} + h_{21} - h_{23} \sin(\theta_2 - \theta_1) \sin(\theta_3 - \theta_2)) \\ \star \\ -h_{32}h_{21} \cos(\theta_1 - \theta_2) \cos(\theta_2 - \theta_3) \end{bmatrix},$$

with $\star = h_{21}(h_{12} \sin^2(\theta_2 - \theta_1) + h_{21} + 2h_{23} \sin(\theta_1 - \theta_2) \sin(\theta_3 - \theta_2) - h_{12} \cos^2(\theta_2 - \theta_1))$. To linearize the Kuramoto network around $\bar{\theta}$, we must compute the linearizing feedback $u = \alpha(\theta) + \beta(\theta)v$, where $\alpha(\theta)$ and $\beta(\theta)$ can be derived

³That is, the weight associated with the edge (j, i) in the inference diagram adjacency matrix is set to 1 if $h_{ij} > 0$, and zero otherwise.

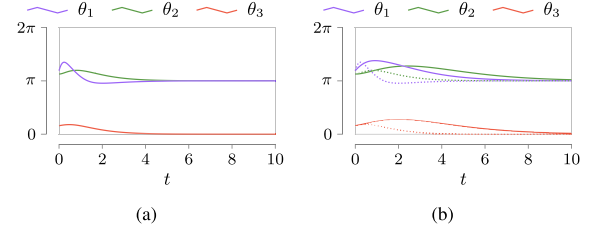


Fig. 5. These figures show phases evolution for the three oscillators in Fig. 4 in a reference framework that rotates with natural frequency ω . (a) The convergence of the phases to the equilibrium $\bar{\theta} = [\pi \ \pi \ 0]^T$ after a stabilizing feedback $v = -Kz$ is applied to the system. The eigenvalues for the matrix $A_{\text{lin}} + bK$ are -1 , -2 , and -3 , which are obtained with the feedback gains $K = [6 \ 11 \ 6]$. (b) The different convergence rates associated with different eigenvalues of $A_{\text{lin}} + bK$. The dotted lines represent the phases of the three oscillators when the eigenvalues are the same as in (a), whereas the solid lines are associated with eigenvalues -0.6 , -0.7 , and -0.8 , and hence with slower dynamics.

from [3, Sec. 4]: $\alpha(\theta) = -\frac{L_f^n \Phi_1}{L_b L_f^{n-1} \Phi_1}$, $\beta(\theta) = \frac{1}{L_b L_f^{n-1} \Phi_1}$, with $\Phi_i(\theta) = L_f^{i-1} \Phi_1(\theta)$, and $\Phi_1(\theta)$ is such that

$$\frac{\partial \Phi_1}{\partial \theta} b = 0, \quad \frac{\partial \Phi_1}{\partial \theta} \text{ad}_f b = 0, \quad \text{and} \quad \frac{\partial \Phi_1}{\partial \theta} \text{ad}_f^2 b \neq 0. \quad (6)$$

The choice $\Phi_1(\theta) = z_1 = \theta_3$ satisfies (6), and yields $L_b L_f^2 \Phi_1 = h_{21}h_{32} \cos(\theta_1 - \theta_2) \cos(\theta_2 - \theta_3)$. From the latter, we derive $\alpha(\theta)$ and $\beta(\theta)$, which we omit here in the interest of space. As a proof of concept, we can easily compute the state space region where the feedback-linearized system is defined. Such a region corresponds to the open set $\{\theta : |\theta_i - \bar{\theta}_i| < \frac{\pi}{2} \text{ for all } i\}$, the boundary points of whose closure are the only coordinates for which $\alpha(\theta)$ and $\beta(\theta)$ are not defined. Finally, we can assign the poles of $\dot{z} = A_{\text{lin}} z + B_{\text{lin}} v$ via classical static feedback $v = -Kz$ (see Fig. 5).

B. Multiplex Network With Multi-Body Interactions

Multiplex networks explicitly incorporate multiple channels of connectivity in a system. In the following, we study a 2-layer multiplex network where the two layers contain neurons with three- and two-body interaction, respectively [33], [34]. Importantly, three-body interactions are thought to play a crucial role in heterosynaptic plasticity [35]. We represent neurons as oscillatory units that obey the dynamics

$$\begin{aligned} \dot{\theta}_i &= \omega + \frac{\kappa_1}{m^2} \sum_{j=1}^m \sum_{k=1}^m \sin(\theta_j + \theta_k - 2\theta_i), \\ \dot{\varphi}_i &= \omega + \frac{\kappa_2}{m} \sum_{j=1}^m \sin(\varphi_j - \varphi_i) + d \sin(\theta_i - \varphi_i), \end{aligned} \quad (7)$$

where ω is the natural frequency, and $\kappa_1, \kappa_2, d \in \mathbb{R}_{>0}$ are coupling strengths. We choose $m = 3$ and we apply a control input to the θ layer of the network (see Fig. 6(a)), so that $B = [e_1, e_2, e_3]$. Further, we fix the constants $\kappa_1 = \kappa_2 = d = 1$. By writing the state of the network as $x = [\theta_1 \ \theta_2 \ \theta_3 \ \varphi_1 \ \varphi_2 \ \varphi_3]^T$, it can be shown that $\bar{x} = [\pi \ \pi \ \pi \ 0 \ 0 \ 0]^T$ is an unstable equilibrium point of (7). It holds that $J(\bar{x}) = [\text{diag}(-d, -d, -d) \otimes 1]$.

Hence, the condition in Theorem 1 is satisfied and the system is feedback-linearizable at \bar{x} . Along the lines of [3,

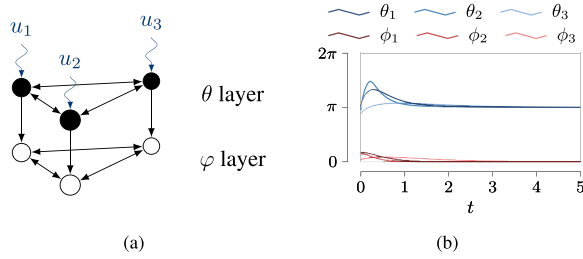


Fig. 6. (a) The 2-layer multiplex network studied in Section IV-B. The θ layer consists of neurons connected with three-body interactions, whereas the φ layer consists of neurons connected with two-body interactions. (b) The convergence of the system's state to the desired point after feedback linearization. The eigenvalues of $A_{\text{lin}} + B_{\text{lin}}K$ are assigned to the left half plane, thus making $\bar{x} = [\pi \ \pi \ \pi \ 0 \ 0 \ 0]^T$ locally stable in the reference frame rotating with velocity ω .

Proof of Lemma 5.2.2], we compute the dummy output functions $\lambda_1(x) = \varphi_1$, $\lambda_2(x) = \varphi_2$, and $\lambda_3(x) = \varphi_3$, from which we obtain the local change of coordinates $\phi_k^i(x) = L_f^{k-1} \lambda_i(x)$, $1 \leq k \leq 2$, $1 \leq i \leq 3$, and finally the linearizing feedback law [3, Sec. 5]. The code for this simulation can be downloaded at [36]. In Fig. 6(b), the computed feedback partitions the network into two distinct clusters. This result extends existing work on the control of cluster synchronization in networks of nonlinearly-interacting oscillators (see, e.g., [8]) to more complex types of interactions.

V. CONCLUSION AND FUTURE DIRECTIONS

We have derived sufficient structural conditions to test for feedback-linearizability of large-scale nonlinear network systems. These conditions also constitute a test for local controllability. The results contained in this letter are particularly suited for large networks, such as multi-agent systems, neuronal networks, and artificial neural networks.

Because of striking topological similarities, future research could investigate the link between feedback-linearizable and strongly structurally controllable networks [37]. Finally, another interesting research direction is the characterization of the gap between locally controllable and feedback-linearizable systems [38].

REFERENCES

- [1] F. Dörfler, M. Chertkov, and F. Bullo, "Synchronization in complex oscillator networks and smart grids," *Proc. Nat. Acad. Sci. USA*, vol. 110, no. 6, pp. 2005–2010, 2013.
- [2] S. Gu *et al.*, "Controllability of structural brain networks," *Nat. Commun.*, vol. 6, Oct. 2015, Art. no. 113171W.
- [3] A. Isidori, *Nonlinear Control Systems* (Communications and Control Engineering Series), 3rd ed. London, U.K.: Springer, 1995.
- [4] A. J. Krener, "On the equivalence of control systems and the linearization of nonlinear systems," *SIAM J. Control*, vol. 11, no. 4, pp. 670–676, 1973.
- [5] J. Sun and A. E. Motter, "Controllability transition and nonlocality in network control," *Phys. Rev. Lett.*, vol. 110, no. 20, 2013, Art. no. 208701.
- [6] C. O. Aguilar and B. Ghahserifard, "Necessary conditions for controllability of nonlinear networked control systems," in *Proc. Amer. Control Conf.*, Jun. 2014, pp. 5379–5383.
- [7] R. F. Betzel and D. S. Bassett, "Multi-scale brain networks," *NeuroImage*, vol. 160, pp. 73–83, Oct. 2017.
- [8] T. Menara, G. Baggio, D. S. Bassett, and F. Pasqualetti, "A framework to control functional connectivity in the human brain," in *Proc. IEEE Conf. Decis. Control*, Nice, France, Dec. 2019, pp. 4697–4704.
- [9] G. Conte, C. H. Moog, and A. M. Perdon, *Algebraic Methods for Nonlinear Control Systems*. London, U.K.: Springer, 2007.
- [10] I. Mir, H. Taha, S. A. Eisa, and A. Maqsood, "A controllability perspective of dynamic soaring," *Nonlinear Dyn.*, vol. 94, no. 4, pp. 2347–2362, 2018.
- [11] A. J. Whalen, S. N. Brennan, T. D. Sauer, and S. J. Schiff, "Effects of symmetry on the structural controllability of neural networks: A perspective," in *Proc. Amer. Control Conf.*, Boston, MA, USA, 2016, pp. 5785–5790.
- [12] I. Klickstein, A. Shirin, and F. Sorrentino, "Locally optimal control of complex networks," *Phys. Rev. Lett.*, vol. 119, Dec. 2017, Art. no. 268301.
- [13] M. T. Angulo, A. Aparicio, and C. H. Moog, "Structural accessibility and structural observability of nonlinear networked systems," *IEEE Trans. Netw. Sci. Eng.*, early access.
- [14] Y. Kawano and M. Cao, "Structural accessibility and its applications to complex networks governed by nonlinear balance equations," *IEEE Trans. Autom. Control*, vol. 64, no. 11, pp. 4607–4614, Nov. 2019.
- [15] E. D. Sontag, "Controllability is harder to decide than accessibility," *SIAM J. Control Optim.*, vol. 26, no. 5, pp. 1106–1118, 1988.
- [16] R. W. Brockett, "Feedback invariants for nonlinear systems," in *Proc. Int. Congr. Math.*, Helsinki, Finland, 1978, pp. 1115–1120.
- [17] B. Jakubczyk and W. Respondek, "On linearization of control systems," *Bull. de l'Académie Polonaise des Sci.*, vol. 28, nos. 9–10, pp. 517–522, 1980.
- [18] B. d'Andréa Novel, G. Campion, and G. Bastin, "Control of nonholonomic wheeled mobile robots by state feedback linearization," *Int. J. Robot. Res.*, vol. 14, no. 6, pp. 543–559, 1995.
- [19] E. Barany, S. Schaffer, K. Wedeward, and S. Ball, "Nonlinear controllability of singularly perturbed models of power flow networks," in *Proc. IEEE Conf. Decis. Control*, vol. 5, Dec. 2004, pp. 4826–4832.
- [20] P. Tabuada, W.-L. Ma, J. W. Grizzle, and A. D. Ames, "Data-driven control for feedback linearizable single-input systems," in *Proc. IEEE Conf. Decis. Control*, Dec. 2017, pp. 6265–6270.
- [21] T. Westenbroek *et al.*, "Feedback linearization for unknown systems via reinforcement learning," 2019. [Online]. Available: arXiv:1910.13272.
- [22] B. Charlet, J. Lévine, and R. Marino, "Sufficient conditions for dynamic state feedback linearization," *SIAM J. Control Optim.*, vol. 29, no. 1, pp. 38–57, 1991.
- [23] L. A. Marquez-Martinez and C. H. Moog, "Input–output feedback linearization of time-delay systems," *IEEE Trans. Autom. Control*, vol. 49, no. 5, pp. 781–785, May 2004.
- [24] X. Liu and T. Chen, "Synchronization of nonlinear coupled networks via aperiodically intermittent pinning control," *IEEE Trans. Neural Netw. Learn. Syst.*, vol. 26, no. 1, pp. 113–126, Jan. 2015.
- [25] P. S. Skardal and A. Arenas, "Control of coupled oscillator networks with application to microgrid technologies," *Sci. Adv.*, vol. 1, no. 7, 2015, Art. no. e1500339.
- [26] Y.-Y. Liu, J.-J. Slotine, and A.-L. Barabási, "Observability of complex systems," *Proc. Nat. Acad. Sci. USA*, vol. 110, no. 7, pp. 2460–2465, 2013.
- [27] H. Nijmeijer and A. Van der Schaft, *Nonlinear Dynamical Control Systems*, vol. 175. New York, NY, USA: Springer, 1990.
- [28] T. Menara, G. Baggio, D. S. Bassett, and F. Pasqualetti, "Stability conditions for cluster synchronization in networks of heterogeneous Kuramoto oscillators," *IEEE Trans. Control Netw. Syst.*, early access.
- [29] T. Menara, G. Baggio, D. S. Bassett, and F. Pasqualetti, "Exact and approximate stability conditions for cluster synchronization of Kuramoto oscillators," in *Proc. Amer. Control Conf.*, Philadelphia, PA, USA, Jul. 2019, pp. 205–210.
- [30] K. Lehnertz *et al.*, "Synchronization phenomena in human epileptic brain networks," *J. Neurosci. Methods*, vol. 183, no. 1, pp. 42–48, 2009.
- [31] C. Hammond, H. Bergman, and P. Brown, "Pathological synchronization in Parkinson's disease: Networks, models and treatments," *Trends Neurosci.*, vol. 30, no. 7, pp. 357–364, 2007.
- [32] J. Cabral, E. Hugues, O. Sporns, and G. Deco, "Role of local network oscillations in resting-state functional connectivity," *Neuroimage*, vol. 57, no. 1, pp. 130–139, 2011.
- [33] A. E. Sizemore, C. Giusti, A. E. Kahn, J. M. Vettel, R. F. Betzel, and D. S. Bassett, "Cliques and cavities in the human connectome," *J. Comput. Neurosci.*, vol. 44, no. 1, pp. 115–145, Feb. 2018.
- [34] P. S. Skardal and A. Arenas, "Abrupt desynchronization and extensive multistability in globally coupled oscillator simplexes," *Phys. Rev. Lett.*, vol. 122, no. 24, 2019, Art. no. 248301.
- [35] J. J. O'Connor, M. J. Rowan, and R. Anwyl, "Long-lasting enhancement of NMDA receptor-mediated synaptic transmission by metabotropic glutamate receptor activation," *Nature*, vol. 367, no. 6463, p. 557, 1994.
- [36] *Matlab Code*. [Online]. Available: <https://github.com/tommasomenara/feedbacklinearization>
- [37] T. Menara, G. Bianchin, M. Innocenti, and F. Pasqualetti, "On the number of strongly structurally controllable networks," in *Proc. Amer. Control Conf.*, Seattle, WA, USA, 2017, pp. 340–345.
- [38] W. Respondek and I. A. Tall, "Nonlinearizable single-input control systems do not admit stationary symmetries," *Syst. Control Lett.*, vol. 46, no. 1, pp. 1–16, 2002.